# Diurnal Variation of Marine Stratocumulus over San Nicolas Island during July 1987

MIRIAM BLASKOVIC AND ROGER DAVIES

*Department of Meteorology, McGill University, Montreal, Quebec, Canada*

J. B. SNIDER

*NOAA/ERL/Wave Propagation Laboratory, Boulder, Colorado*

(Manuscript received 21 May 1990, in final form 4 December 1990)

ABSTRACT

Surface measurements made at San Nicolas Island during the intensive field observation marine stratocumulus phase of the First International Satellite Cloud Climatology Program Regional Experiment, July 1987, are analyzed to retrieve the average diurnal variation of marine stratocumulus and related surface variables. Cloud thickness and integrated liquid-water content show a clear decrease during the day from sunrise to sunset, increasing thereafter. The average liquid-water density in the cloud is closely related to the cloud thickness, decreasing as the cloud thickness decreases. The cloud-base height has a diurnal range of 150 ± 30 m, rising from sunrise till midafternoon. The cloud-top height has a similar diurnal range of 130 ± 30 m, but the main descent occurs in the late afternoon. Surface air temperature also increases at sunrise, directly in phase with the cloud-base lifting, and has a diurnal range of 2°C.

The diurnal behavior of the cloud base appears to be consistent with model-predicted uncoupling of the cloud layer and the subcloud layer as the turbulent flux of moisture is inhibited by solar heating near the cloud base. Similarly, variation in surface air temperature is consistent with the inhibition of the turbulent flux of heat between the two layers, shielding the surface from the effect of longwave cooling from the cloud top. The variation in cloud-top height, however, does not appear to be readily explainable by present diurnal models.

## 1. Introduction

The presence or absence of cloud has an understandably important effect on planetary and surface radiation budgets. This importance is in no way diminished in the case of low-level marine stratocumulus. These clouds cover large areas of the global oceans and contribute a significant measure of shortwave cloud forcing (Ramanathan et al. 1989) that is relatively uncompensated by longwave forcing, due to high albedo contrast and low temperature contrast between cloud and ocean. The net radiation budget of the earth is therefore significantly reduced when these clouds are present, and the ability to understand the factors that influence their presence or absence is a desirable step towards a comprehensive theory of the earth's climate system.

Despite occurring over the oceans in regions of large-scale subsidence, marine stratocumulus show an interesting diurnal variation (Minnis and Harrison 1984). The general characteristic is an increase in cloud cover during the night and a decrease during the day. Diurnal cloud behavior is generally rather difficult to treat in climate models, results from which can be sensitive to the treatment of diurnal effects (Wilson and Mitchell 1986). Modeling the physical processes governing the diurnal variation of stratocumulus appears to be particularly challenging.

While diurnal variability must, in general, be initiated by the absorption of solar radiation, and some solar radiation is certainly absorbed by marine stratocumulus, the amount absorbed by the entire cloud seldom exceeds the radiation lost by longwave emission from the cloud top. [See Davies et al. (1984) for examples of absorbed solar radiation, and Davies and Alves (1989) for examples of emitted longwave radiation.] The diurnal behavior of the cloud is not, therefore, a directly proportionate response to solar absorption and appears to involve at least one other intermediate mechanism.

Neither can the diurnal variation be explained in terms of land- or sea-breeze effects, as it remains equally evident far from land (Minnis and Harrison 1984). Surface forcing is also an unlikely explanation. For example, an average diurnal range in sea surface temperatures of 0.24°C was measured at a latitude of ≈15°N in the Atlantic Ocean during BOMEX, under generally fair sky conditions (Delnore 1972). This diurnal range would presumably be even smaller in the presence of persistent stratocumulus.

*Corresponding author address:* Dr. Roger Davies, Associate Professor, Dept. of Meteorology, McGill University, 805 Sherbrooke Street West, Montreal, Quebec H3A 2K6, CANADA

The explanation for the diurnal cloud behavior appears to depend on the perturbation of the turbulent flux of moisture that sustains the cloud in regions of large-scale subsidence. The cloud composition is most likely determined by a complicated interaction between radiation, microphysics, and turbulence, with each of these processes responding to changes in the cloud composition in a feedback system that may be tightly coupled. Several numerical models have been developed (Bougeault 1985; Turton and Nicholls 1987; Duynkerke and Driedonks 1987, for example) which simulate aspects of this behavior.

They illustrate the relative role of the shortwave heating and longwave cooling profiles within the cloud. The longwave net flux divergence is locally significant over the uppermost portion of the cloud only. At a depth of 50–100 m below the cloud top this divergence is usually insignificant, and at the cloud base it is usually weakly negative (the amount depending mainly on the temperature contrast between cloud base and surface). Shortwave absorption is also greatest at the cloud top, where it is typically much lower in magnitude than the longwave net flux divergence, but it decreases less rapidly with depth into the cloud. As a result, a diurnally varying radiative net flux convergence (tending to warm the cloud) occurs locally at some distance below the cloud top. The previously mentioned models illustrate that this local radiative heating may lead to an uncoupling of the cloud layer from the subcloud layer. This uncoupling can inhibit the turbulent transfer of moisture to the cloud, resulting in systematic thinning or dissipation of the cloud layer under the influence of the background subsidence. However, the radiative relaxation times are longer than the usually assumed convective or turbulent time constants for equivalent layer thicknesses, and our present knowledge of the physics of this radiation modulation remains, at least quantitatively, incomplete.

This paper examines the observational evidence for the diurnal variation of marine stratocumulus that was collected during a period of intensive field observations (IFOs) as part of the First ISCCP (International Cloud Climatology Program) Regional Experiment (FIRE). As described in detail by Albrecht et al. (1988), the field site for the FIRE marine stratocumulus IFO was located on the extreme upwind end of San Nicolas Island (33.1°N,119.31°W, approximately 100 km southwest of Los Angeles) such that the data collected were relatively unperturbed by island effects and were characteristic of marine conditions. Of interest to the present study was the combination of a variety of instruments, which were well suited to providing information on the time dependent nature of marine stratocumulus and made more or less continuous measurements between 1 July and 19 July 1987.

Data collection by these instruments is described next, followed by an analysis of the average diurnal behavior of marine stratocumulus and the relevant surface variables during the period of the FIRE IFO. We conclude with a brief discussion of how the results from this analysis relate to the above explanation of a solar control of turbulent fluxes between the cloud and subcloud layers.

## 2. Summary of field observations

In order to study the time evolution of clouds and the related marine boundary-layer structure during the marine stratocumulus IFO periods of FIRE, continuous measurements were made of several variables with high temporal resolution. A number of instruments operated concurrently; the characteristics of which are summarized in Table 1. Of main relevance to the present study are data collected by the Doppler acoustic sounder (sodar), the laser ceilometer, and the microwave radiometer. These three instruments were located within close proximity of each other (the ceilometer was located 14 m above sea level, 20 m west of the radiometer, and 40 m north of the acoustic sounder), so that their measurements refer to similar, if not exactly identical, sections of the cloud.

Cloud-top height was determined indirectly by a Xondar III Doppler acoustic sounder (sodar) operated by The Pennsylvania State University, as analyzed by White (1989). This instrument measures the reflectivity profile of the structure coefficient, which in turn serves as a proxy indicator of the temperature inversion height associated with the cloud top. Comparison on a point-by-point basis with profiles taken using CLASS radiosondes confirmed that the cloud-top height was in close agreement with the temperature inversion height as measured by the sodar. The sodar measurements were made available to us in the form of hourly averages, and this limited the time resolution of cloud-top height and derived products to hourly values.

Cloud-base height was determined directly from a Vaisala CT 12K laser ceilometer operated by Colorado State University, as described by Schubert et al. (1987). This instrument operated continuously and provided the height of the cloud base (or identified an absence of cloud) at 30-s intervals.

Integrals of the column amount of water-vapor and liquid-water content were measured by a 3-channel (20.6, 31.65, and 90.0 GHz) microwave radiometer

TABLE 1. Summary of data availability from different surface instruments during the FIRE IFO.

| Instrument | Operational (1987) | Data availability |
|---|---|---|
| Sodar | 1 July–19 July | Hourly |
| Ceilometer | 1 July–19 July | 30 s |
| Radiometer | 1 July–19 July | 60 s |
| Radiosonde | 30 June–19 July | Variable (from once to nine times per day) |

operated by the Wave Propagation Laboratory (WPL) of NOAA as described by Hogg et al. (1983). A statistical algorithm converts recorded brightness temperatures of the atmosphere into amounts of water vapor and liquid water. In this paper we consider only the liquid-water observations that were retrieved from brightness temperatures measured at the two lower operating frequencies. The absolute accuracy of the two-channel liquid measurement is estimated to be 20%. However, comparison of radiometric liquid measurements at San Nicolas Island with calculations of adiabatic values (Albrecht et al. 1990) suggests that the accuracy is better than the estimated value. The sensitivity of the microwave radiometer to short-term fluctuations is approximately 0.005 mm. The WPL radiometer yielded nearly continuous measurements throughout the IFO period with a time resolution of 1 min. For this experiment, we attribute the column liquid-water amount entirely to the boundary-layer stratocumulus, noting that the subsidence during the IFO led to an absence of liquid-water clouds above the stratocumulus, and that the ice-water content of cirrus clouds is not detected at the frequencies employed by the WPL radiometer.

## 3. Data analysis

The diurnal averaging involved three types of data: high resolution (sampling time $\approx$ 1 min), low resolution (sampling or averaging time $\approx$ 1 h), and derived products. The high-resolution data analyzed here include ceilometer, radiometer, surface pressure, and surface air temperature measurements, each of which were first averaged over 60 s. Low-resolution data include cloud-top height, surface wind speed, surface wind direction, and surface insolation. Derived products include cloud thickness and average liquid-water density.

The time series for each variable was carefully checked for any spurious points. For the ceilometer data, only measurements of a well-defined cloud base were used. Similarly, only integrated liquid amounts greater than zero were used in the analysis of the radiometer data.

The diurnal variability of a short meteorological time series can easily be obscured by secular trends due to synoptic changes. Fortunately, synoptic disturbances during the IFO were minor. Extensive low-level clouds covered much of the eastern Pacific in association with a persistent high pressure system located off the Californian coast (Kloesel et al. 1988), and a very weak low pressure trough moved across the observation site on 10 July with little effect other than a pressure change. Under these conditions, the mean diurnal variability of each variable could have been retrieved with fair accuracy simply by direct averaging as a function of local time. However, we chose a procedure that yielded superior diurnal results by objectively removing the effects of long-term secular trends. For each hourly value, the departure from the 24-h running mean centered on that value was calculated first. All such departures for each local solar time were then averaged and the mean departure finally added to the overall mean of the total record to produce the diurnal plots shown in the following.

Evidence that this analysis eliminated synoptic trends is given by the mean diurnal variability of surface pressure, results for which are shown in Fig. 1 for a time resolution of 1 min. The semidiurnal pressure tide is clearly visible. All other high-resolution data were analyzed similarly.

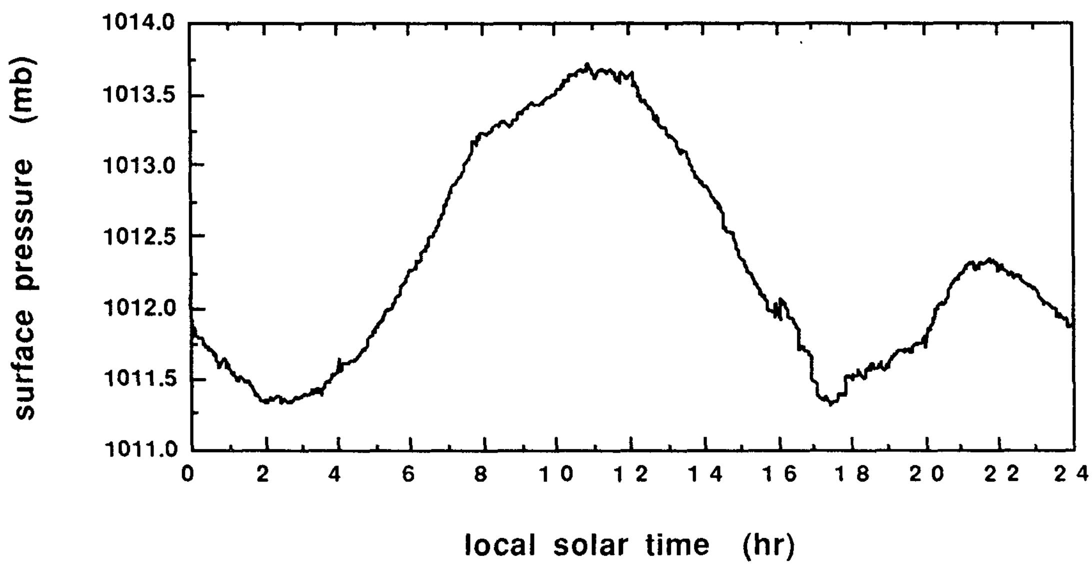


FIG. 1. Diurnal variation of surface pressure at San Nicolas Island during the FIRE IFO.

TABLE 2. Number of available values corresponding to each local hour, for the cloud base, cloud top, and column liquid analyses.

| Hour | 1 | 2 | 3 | 4 | 5 | 6 | 7 | 8 | 9 | 10 | 11 | 12 | 13 | 14 | 15 | 16 | 17 | 18 | 19 | 20 | 21 | 22 | 23 | 24 |
|---|---|---|---|---|---|---|---|---|---|---|---|---|---|---|---|---|---|---|---|---|---|---|---|---|
| Base | 14 | 14 | 15 | 15 | 15 | 14 | 15 | 15 | 14 | 14 | 15 | 14 | 14 | 14 | 12 | 12 | 11 | 11 | 12 | 12 | 12 | 13 | 14 | 14 |
| Top | 12 | 11 | 12 | 13 | 13 | 13 | 13 | 13 | 13 | 12 | 12 | 12 | 13 | 12 | 12 | 13 | 14 | 13 | 13 | 12 | 14 | 14 | 14 | 13 |
| Liquid | 15 | 16 | 17 | 16 | 16 | 17 | 17 | 16 | 14 | 14 | 15 | 14 | 14 | 12 | 11 | 13 | 11 | 11 | 14 | 14 | 12 | 14 | 15 | 15 |

Analysis of the data with a time resolution of 1 h followed the same format. When high-resolution data, namely, cloud-base height and cloud liquid water, were needed for direct comparison with low-resolution data, they were first degraded to low resolution by averaging over an hour. There was a possible maximum of 19 values for each of the 24 hourly departures. In practice, however, if no cloud was present or if an instrument failed to provide an accurate hourly value, this number was of course lower. The total number of data points for each of the 24 mean hourly values is summarized for the cloud variables in Table 2.

In determining the derived quantities, our procedure was first to average the values of the independent variables and then to calculate the dependent variable. This is particularly important in the determination of liquid water density, which depends nonlinearly upon the cloud-base height, cloud-top height, and column liquid-water amount. Direct averaging of the dependent variable would have yielded spurious results due to nonlinear application of the noise present in the input variables.

Natural variability in all the datasets was accounted for by treating the data as independent from one day to the next, and using normal statistics to estimate the error in the mean based on the sample variance. The error bars plotted in the subsequent figures reflect the 1-$\sigma$ estimate of this error in the mean hourly values.

## 4. Results

The mean diurnal behavior of the column liquid-water content of the atmosphere (Fig. 2) shows a steady decrease from midmorning to late afternoon, and a systematic rise thereafter. The double peak either side of sunrise is not characteristic of the diurnal behavior but can be traced to particularly high values on two days.

Figure 3 shows the high-resolution diurnal averages of the cloud-base height. Hourly averages of the same data are given in Fig. 4, together with the expected error in the mean hourly values. The main diurnal behavior stands out clearly from the noise, namely, that the base rises during the day from about 0500 LST (i.e., local sunrise) until midafternoon, after which it falls steadily until the following sunrise. Details of the ascent and descent rates are more ambiguous due to noise, but there appears to be an increase in the lifting rate around 1000 LST, and a decrease in the descent rate around 1900 LST (sunset). The diurnal range of the cloud-base height averages 150 ± 30 m.

Figure 4 summarizes the main cloud properties on an hourly basis, showing cloud-top and cloud-base heights. The cloud top behaves differently from the base, lifting in the early morning to a peak altitude around 1000 LST and then lowers to a minimum altitude around 2000 LST. The descent rate of the cloud

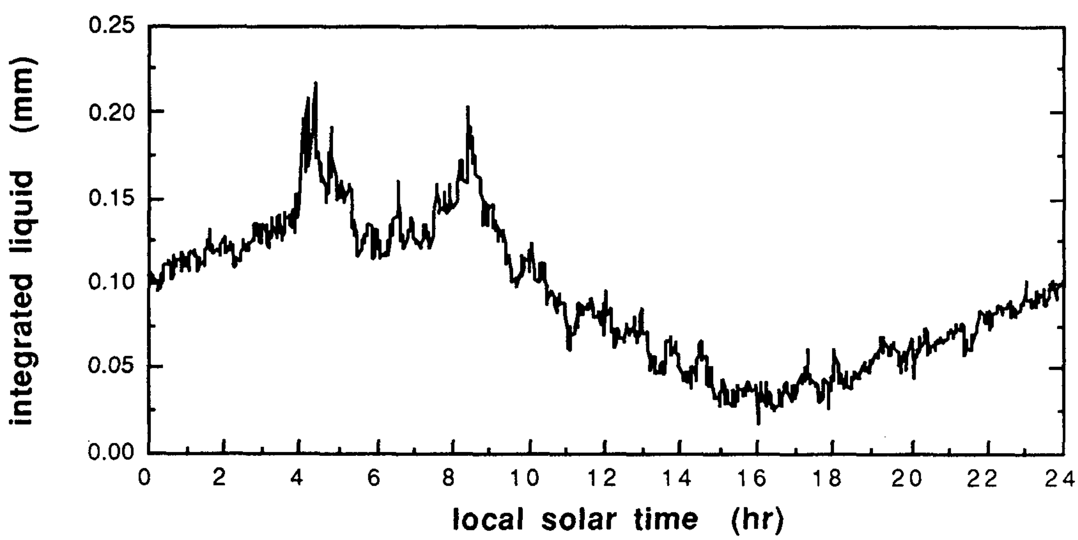


FIG. 2. The diurnal variation of column integrated liquid-water content.

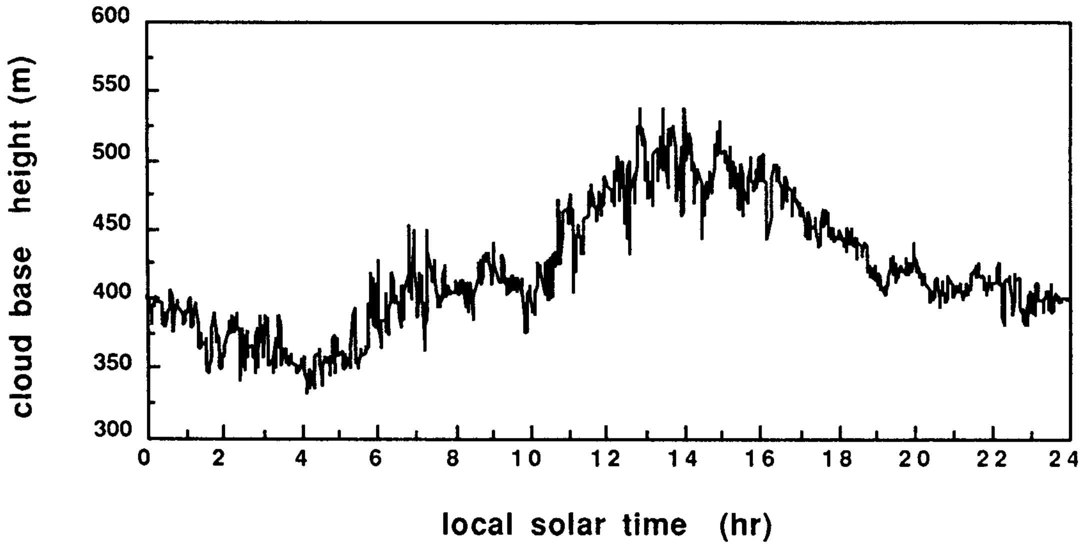


FIG. 3. The diurnal variation of cloud-base height.

top is greatest in the late afternoon, at the same time as the base is also lowering. The diurnal range of the cloud-top height averages 130 ± 30 m.

The average cloud liquid-water density, derived from the column liquid-water content and the cloud thickness, is shown in Fig. 5. It peaks around sunrise and decreases throughout the day until late afternoon, varying in magnitude from 0.7 ± 0.2 to 0.25 ± 0.09 g $m^{-3}$.

An approximate linear relationship between liquid-water density and cloud thickness is evident once the data have been averaged over the entire observing period. Figure 6 shows the 24 points obtained from each of the local hour values, together with the result of a linear regression between liquid-water density and cloud thickness.

Figure 7 shows that the mean diurnal range of surface air temperature is about 2°C. Note the similarity in

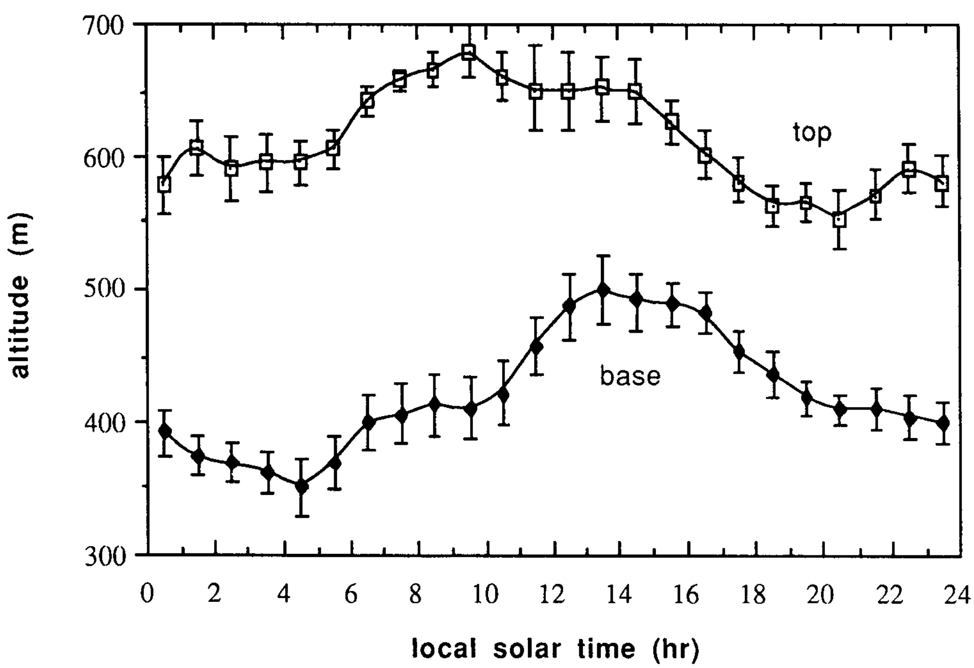


FIG. 4. The diurnal variation of cloud-top and cloud-base heights.

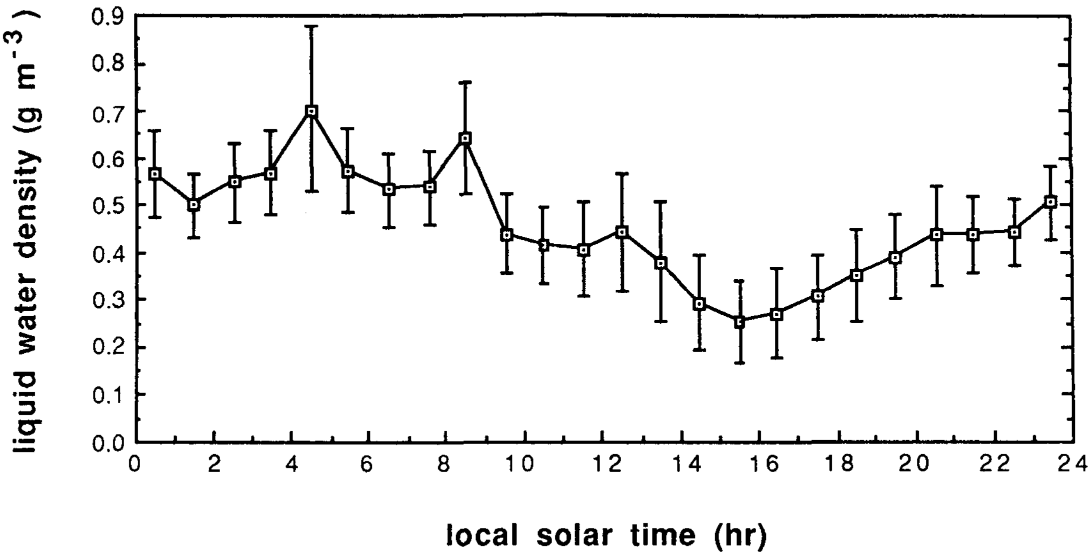


FIG. 5. The diurnal variation of mean liquid-water density.

the average diurnal variation of temperature and cloud-base height (Figs. 7 and 3, respectively). Both show a sharp change about local sunrise, increasing to a maximum around 1500 LST, with slower changes after sunset.

Other diurnal changes of interest include surface wind speed (Fig. 8), wind direction (Fig. 9), and broadband solar insolation (Fig. 10). The wind speed shows an interesting decrease throughout the night, reaching a minimum of 4.5 m $s^{-1}$ by sunrise. Wind direction is 270° between sunrise and 1000 LST, shifts abruptly to 290° at 1000 LST, and varies around 280° between sunset and sunrise. Solar insolation is asymmetric with respect to local solar noon, showing relatively higher values in the afternoon compared with the morning.

## 5. Discussion

Despite the relatively short observing period of the FIRE IFO, a number of conclusions can be drawn about the diurnal behavior of marine stratocumulus.

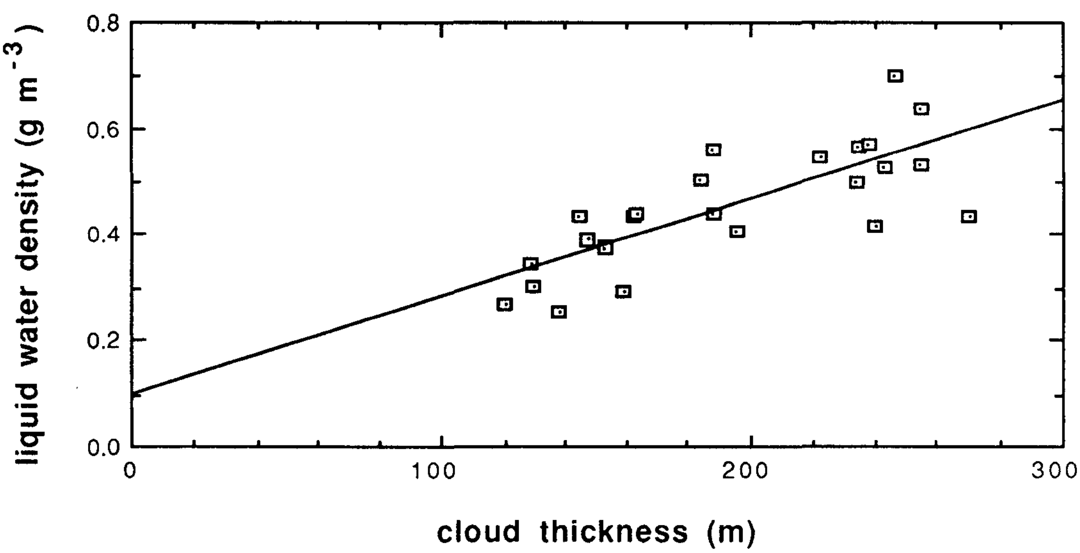


FIG. 6. Scatterplot of average liquid-water density versus cloud thickness, taken from the average results for each hour of local solar time. A linear fit to the data is also shown.

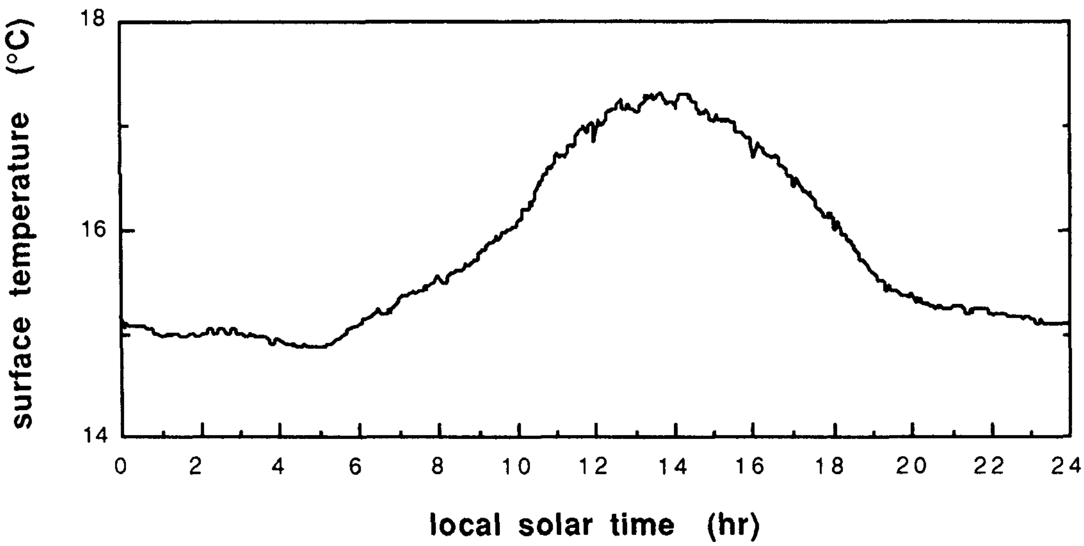


FIG. 7. The diurnal variation of surface air temperature during the FIRE IFO on San Nicolas Island.

Diurnal changes do not follow solar insolation directly, in the sense that they are not cosine weighted symmetrically about local solar noon. Instead, a rapid change in cloud behavior appears to be triggered at local sunrise, characterized by a lifting of the cloud base. At the same time, there is an increase in surface air temperature and the surface wind speed stops decreasing. A second event appears around 1000 LST, characterized by an accelerated lifting of the base, an accelerated rise in surface air temperature, and an increase in surface wind speed. It is at this time also that the cloud top may start to descend, but the descent rate does not appear to be significant until after 1400 LST. The reverse processes are not as clearly marked, with cloud base descending in phase with the decrease in surface air temperature, but preceding the rise in cloud-top height by several hours.

Explanations for some of the diurnal behavior are readily apparent. The surface insolation, for example, is in direct response to the thinning of the cloud, and hence is higher in the afternoon than the morning. The dependence of average liquid-water density on cloud thickness is likely due to a dilution effect near the cloud boundaries. Therefore, the greater the ratio of this edge

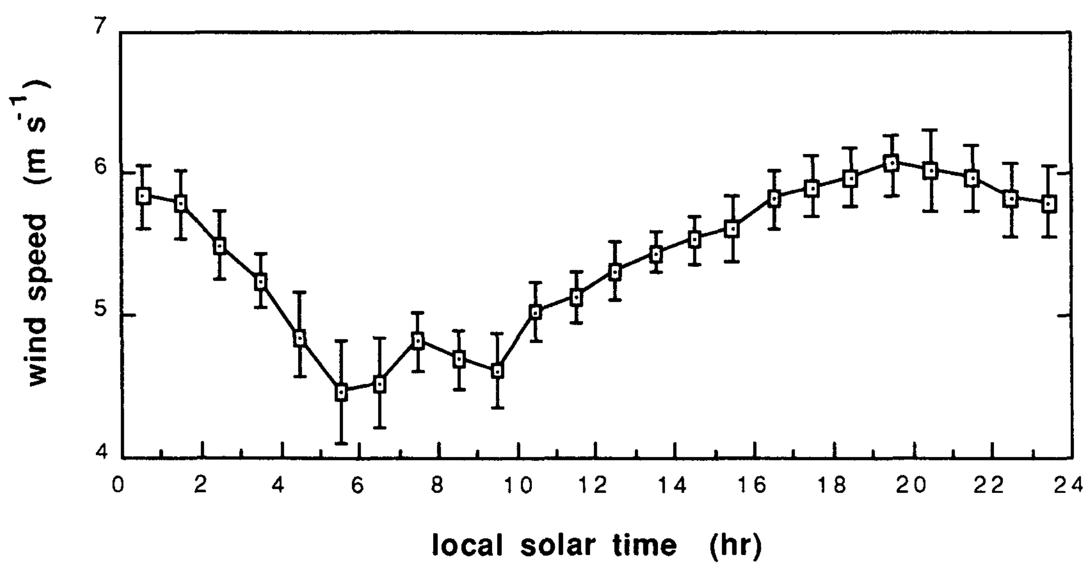


FIG. 8. The diurnal variation of surface wind speed at San Nicolas Island during the FIRE IFO.

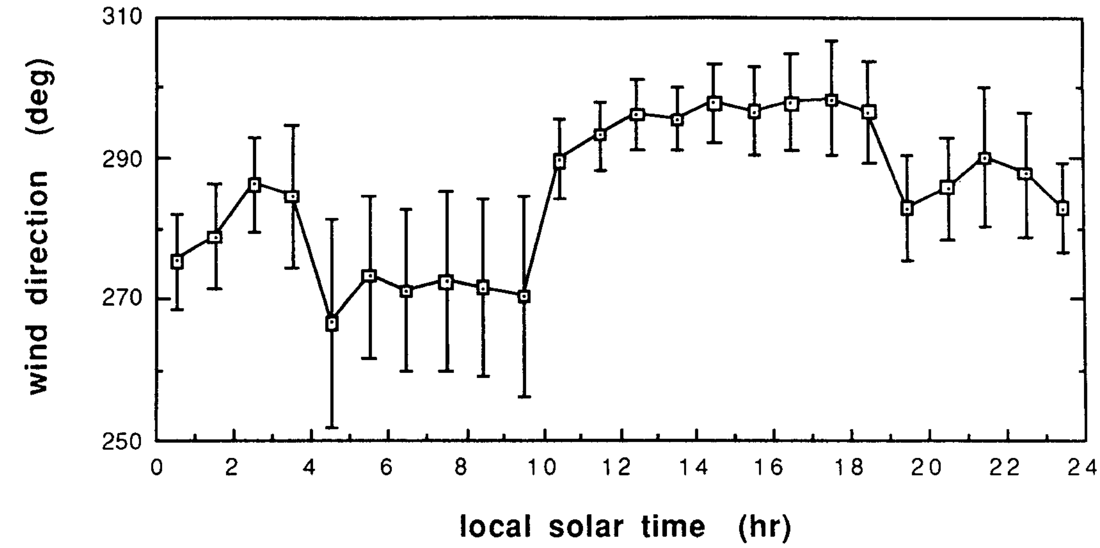


FIG. 9. The diurnal variation of surface wind direction on San Nicolas Island during the FIRE IFO.

effect to the total cloud thickness, the lower the average liquid-water density.

The other effects can be explained less readily, but are consistent with the scenario of turbulent exchange processes being modulated by the absorption of solar radiation near the cloud-layer base. The observed lifting of the cloud base agrees with the associated reduction in moisture flux as modeled, for example, by Turton and Nicholls (1987). We note here that this modulation not only affects the turbulent transfer of moisture to the cloud base, but must also affect the transfer of heat and momentum fluxes at the surface. The cooling effect on the subcloud layer of longwave radiative loss from the cloud top must therefore be diminished simultaneously, and this is why we see a parallel rise in surface air temperature. The observed 2°C diurnal

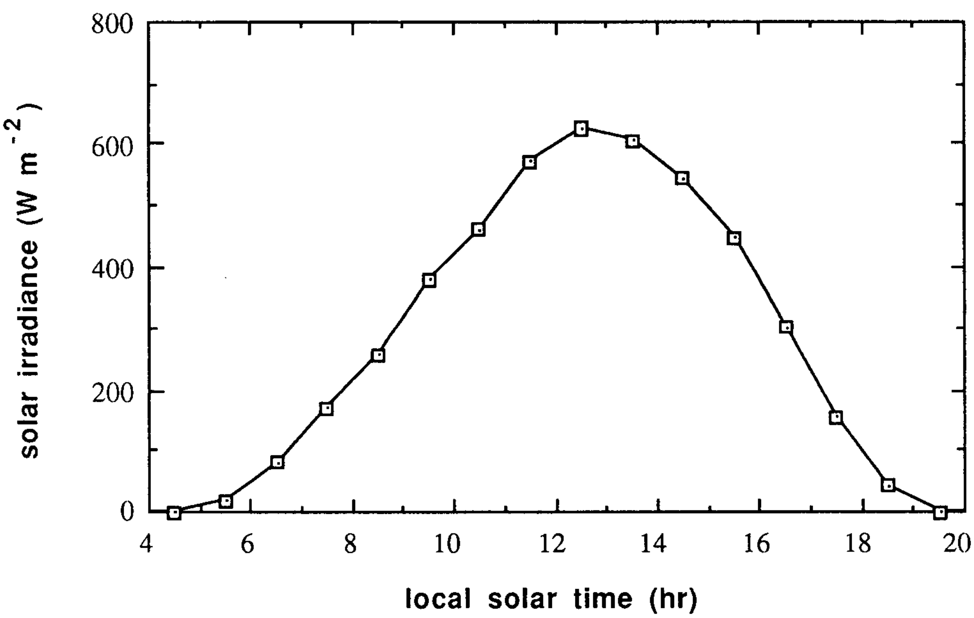


FIG. 10. The diurnal variation of solar irradiance at the surface at San Nicolas Island during the FIRE IFO.

range of surface air temperature appears to be an order of magnitude higher than that expected from solar heating of sea surface temperatures under cloud-free conditions (Delnore 1972), and with an onshore wind of at least 4 m $s^{-1}$ is probably not strongly influenced by surface heating of the island. At the same time, the evaporative flux from the ocean must be diminished. This explanation is also consistent with the sustained decrease in momentum flux transfer at the surface, although this may be coincidental since the surface wind speed has been decreasing steadily prior to sunrise independently of any solar radiation considerations.

It is harder to explain the accelerated lifting of the cloud base around 1000 LST and the sharp descent of the cloud top in the early afternoon. As long as the cloud and subcloud layers remain well coupled, the turbulent kinetic energy generated in response to the loss of longwave radiation from the cloud top is distributed throughout both layers. The separation of cloud and subcloud layers at sunrise should limit the subsequent distribution of turbulent kinetic energy to the cloud layer, and presumably the observed changes in the cloud top and base are in response to the increased concentration of this turbulence. Eventually the rise in turbulent kinetic energy within the cloud layer must overcome the separation between the cloud and subcloud layers, allowing the fluxes of moisture and sensible heat to again pass between the two layers, with the joint result that the cloud-base and surface air temperature fall. It appears to take some time before this process affects the cloud top, allowing it to rise again, however, and the relative timing of the cloud-top descent compared with the accelerating lifting of the cloud base remains unexplained. Predicted variation in cloud-top height has not yet been a feature of the double mixed-layer diurnal models. Using a single mixed-layer model, Schubert (1976) did obtain a small ($\approx$50 m) decrease in the cloud-top height during the day, but this was in phase with a decrease in surface air temperature and a lowering of the cloud base.

The preceding explanation is necessarily speculative, and a more quantitative understanding is needed. A question also remains as to the representativeness of this analysis. The diurnal variation of the cloud layer observed at San Nicolas Island is consistent with the results of Minnis and Harrison (1984) for stratocumulus cloud at distances much farther from the coast. However, Syrett (1988) has noted the existence of significant variations in the wind speed and direction at cloud altitude, especially during the first half of the observing period, which are likely to be local phenomena related to the Californian coast north of the island. Clark and Dembeck (1991) also document the presence of a Catalina eddy, which may have added a local coastal influence to the diurnal wind variation at San Nicolas Island during a subset of this period (from 5 July to 12 July). To the extent that the diurnal results presented here have been influenced by such variations in the wind field at cloud altitude, they would of course be unrepresentative of general marine stratocumulus variability. The fact that Betts (1990) found similar diurnal changes in the cloud base and height over only a 2-day period (10–12 July 1987) when these winds were a minimum leads us to expect their influence on our 19-day analysis to be of secondary importance as far as the cloud properties are concerned.

A future field experiment in a different location would nonetheless be desirable, with greater emphasis placed on obtaining time series of the vertical profiles of temperature, wind, and liquid-water density from the surface to the cloud top, as might be obtained from tethered balloons or appropriate remote sensors.

*Acknowledgments.* We are pleased to acknowledge the following data sources: Wayne H. Schubert for the ceilometer measurements of cloud base and radiosonde data; Bruce A. Albrecht and Allan B. White for sodar data; and Christopher W. Fairall for wind speed, wind direction, and solar radiometer data. We are grateful to M. K. Yau and T. Warn for helpful discussions. Partial funding for this research was received from NASA Grant NAG 1-552, NSERC and AES operating grants.

REFERENCES

Albrecht, B. A., D. A. Randall and S. Nicholls, 1988: Observations of marine stratocumulus clouds during FIRE. *Bull. Amer. Meteor. Soc.*, **69**, 618–626.

——, C. W. Fairall, D. W. Thomson, A. B. White, J. B. Snider and W. H. Schubert, 1990: Surface-based remote sensing of the observed and the adiabatic liquid water content of stratocumulus clouds. *Geophys. Rev. Letters*, **17**, 89–92.

Betts, A. K., 1990: Diurnal variation of California coastal stratocumulus from two days of boundary layer soundings. *Tellus*, **42A**, 302–304.

Bougeault, P., 1985: The diurnal cycle of the marine stratocumulus layer: A higher-order model study. *J. Atmos. Sci.*, **42**, 2826–2843.

Clark, J. H. E., and S. R. Dembeck, 1991: The Catalina eddy event of July 1987: A coastally trapped mesoscale response to synoptic forcing. *Mon. Wea. Rev.*, **119**, in press.

Davies, R., and A. R. Alves, 1989: Flux divergence of thermal radiation within stratiform clouds. *J. Geophys. Res.*, **94**, 16 277–16 286.

——, W. L. Ridgway and K.-E. Kim, 1984: Spectral absorption of solar radiation in cloudy atmospheres: A 20 $cm^{-1}$ model. *J. Atmos. Sci.*, **41**, 2126–2137.

Delnore, V. E., 1972: Diurnal variation of temperature and energy budget for the oceanic mixed-layer during BOMEX. *J. Phys. Oceanogr.*, **2**, 239–247.

Duynkerke, P. G., and A. G. M. Driedonks, 1987: A model for the turbulent structure of the stratocumulus-topped atmospheric boundary layer. *J. Atmos. Sci.*, **44**, 43–64.

Hogg, D. C., F. O. Guiraud, J. B. Snider, M. T. Decker and E. R. Westwater, 1983: A steerable dual-channel microwave radiometer for measurement of water vapor and liquid in the troposphere. *J. Climate Appl. Meteor.*, **22**, 789–806.

Kloesel, K. A., B. A. Albrecht and D. P. Wylie, 1988: FIRE marine stratocumulus observations—summary of operations and synoptic conditions. FIRE Tech. Rep. No. 1, Pennsylvania State University, 171 pp. [Available from: The Pennsylvania State University, Dept. of Meteorology, University Park, PA 16802.]

Minnis, P., and E. F. Harrison, 1984: Diurnal variability of regional cloud and clear-sky radiative parameters derived from GOES data. Part II: November 1978 cloud distributions. *J. Climate Appl. Meteor.,* **23,** 1012–1031.

Ramanathan, V., B. R. Barkstrom and E. F. Harrison, 1989: Climate and the earth's radiation budget. *Phys. Today,* **42,** 22–32.

Schubert, W. H., 1976: Experiments with Lilly's cloud-topped mixed-layer model. *J. Atmos. Sci.,* **33,** 436–446.

——, S. K. Cox, P. E. Ciesielski and C. M. Johnson-Pasqua, 1987: Operation of a ceilometer during the FIRE marine stratocumulus experiment. Atmospheric Science Paper No. 420, Colorado State University (FIRE Vol. 3), 34 pp. [Available from: Dept. of Atmospheric Science, Colorado State University, Fort Collins, CO 80523.]

Syrett, W. J., 1988: Hourly wind, potential temperature, and Richardson number profiles at San Nicolas Island during project FIRE. FIRE Tech. Rep. No. 2, Pennsylvania State University, 49 pp. [Available from: The Pennsylvania State University, Dept. of Meteorology, University Park, PA 16802.]

Turton, J. D., and S. Nicholls, 1987: A study of the diurnal variation of stratocumulus using a multiple mixed layer model. *Quart. J. Roy. Meteor. Soc.,* **113,** 969–1009.

White, A. B., 1989: Temperature and humidity structure parameters deduced from sodar and radar reflectivities: An analysis of data from the marine Stratocumulus phase of FIRE. M.S. thesis, Pennsylvania State University, 137 pp. [Available from: The Pennsylvania State University, Dept. of Meteorology, University Park, PA 16802.]

Wilson, C. A., and J. F. B. Mitchell, 1986: Diurnal variation and cloud in a general circulation model. *Quart. J. Roy. Meteor. Soc.,* **112,** 347–369.